Available on CMS information server

CMS NOTE 2011/XXX

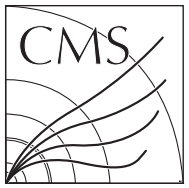

The Compact Muon Solenoid Experiment

CMS Note

Mailing address: CMS CERN, CH-1211 GENEVA 23, Switzerland

September 25, 2012

$\mathrm{E_T^{miss}}$ Templates Results and Additional Cross-checks for the Opposite-sign Same-flavor ("Edge") Dilepton Analysis

D. Barge, C. Campagnari, D. Kovalskyi, V. Krutelyov

University of California, Santa Barbara, USA

W. Andrews, G. Cerati, D. Evans, F. Golf, I. MacNeill, S. Padhi, Y. Tu, F. Würthwein, A. Yagil, J. Yoo

University of California, San Diego, USA

L. Bauerdick, K. Burkett, I. Fisk, Y. Gao, O. Gutsche, B. Hooberman, S. Jindariani, J. Linacre, V. Martinez Outschoorn

Fermi National Accelerator Laboratory, Batavia, Illinois, USA

Abstract

The Aachen and ETH groups have reported an excess of events with low mass, opposite-sign same-flavor lepton pairs, commonly referred to as the "edge analysis." In this note, we use the $\mathrm{E_T^{miss}}$ templates technique to estimate the Z background in the Z mass region for the two signal regions used in this analysis. This prediction is extrapolated to low mass to estimate the γ^*/Z contribution. Additional cross-checks are also presented.

Contents

1 Introduction

The Aachen and ETH groups have reported an excess of events with low mass, opposite-sign same-flavor (OSSF) lepton pairs, as described in AN-2012/200 (Aachen) and An-2012/231 (ETH). In Sec. 2 of this note, we use the $\mathrm{E_T^{miss}}$ templates technique [1] to estimate the Z background in the Z mass region for the two signal regions used in this analysis. This prediction is extrapolated to low mass to estimate the γ^*/Z contribution. In Sec. 3 we cross-check the results of the nominal analysis based on dilepton triggers using single lepton triggers.

2 Results of the $\mathrm{E_T^{miss}}$ Templates Analysis

In this section, we use the $\mathrm{E_T^{miss}}$ templates technique to derive predictions for the Z background in the Z mass regions for the two signal regions used for the OSSF dilepton analysis. The background estimation methodology used in the $\mathrm{E_T^{miss}}$ templates analysis is described in AN-2012/254; this AN presents only details which differ from that reference. We then use the predicted Z background to derive an estimate of the low-mass γ^*/Z contributions, using an extrapolation technique commonly referred to as the "$R_{out/in}$" technique.

2.1 Signal Regions

The two signal regions of the OSSF analysis are defined as:

- Low-$\mathrm{E_T^{miss}}$ signal region (ETH)
  - 2 $p_T > 20$ GeV leptons with $|\eta| < 2.4$
  - At least 3 jets ($p_T > 40$ GeV, $|\eta| < 3$)
  - $\mathrm{E_T^{miss}} > 100$ GeV
- High-$\mathrm{E_T^{miss}}$ signal region (Aachen)
  - leading lepton $p_T > 20$ GeV, trailing lepton $p_T > 10$ GeV, both with $|\eta| < 2.4$
  - At least 2 jets ($p_T > 40$ GeV, $|\eta| < 3$) with scalar sum $H_T > 100$ GeV
  - $\mathrm{E_T^{miss}} > 150$ GeV

2.2 Synchronization Exercise

We perform a synchronization exercise to make sure that we can reproduce the ETH/Aachen results. In Table 1 we display the yields in the Z mass regions of the 2 signal regions and compare these to results from the ETH group. In general we are synchronized to 3% or better in all channels. Note that for the purposes of this exercise we include an additional dimuon trigger (HLT_Mu17_TkMu8) which is not yet included in the results that follow. The inclusion of this trigger adds 3 $\mu\mu$ events in both the low $\mathrm{E_T^{miss}}$ and high $\mathrm{E_T^{miss}}$ signal regions.

Table 1: Summary of the synchronization exercise with the ETH group with 9.2 fb^{-1}. The yields in the Z mass region ($81 < m_{\ell\ell} < 101$ GeV) are displayed for the low $\mathrm{E_T^{miss}}$ and high $\mathrm{E_T^{miss}}$ signal regions.

low $\mathrm{E_T^{miss}}$ signal region	UCSB-UCSD-FNAL	ETH
ee	125	123
$\mu\mu$	166	164
eμ	186	186
high $\mathrm{E_T^{miss}}$ signal region	UCSB-UCSD-FNAL	ETH
ee	75	72
$\mu\mu$	95	94
eμ	113	113

2.3 Background Estimation Methodology

The strategy is to select Z$\rightarrow \ell\ell$ candidates ($81 < m_{\ell\ell} < 101$ GeV) with jet requirements corresponding to the low-$\mathrm{E_T^{miss}}$ and high-$\mathrm{E_T^{miss}}$ signal regions, and compare the observed $\mathrm{E_T^{miss}}$ distribution to the sum of the predictions from the $\mathrm{Z} + \mathrm{jets}$ background (from the $\mathrm{E_T^{miss}}$ templates method based on the $\gamma + \mathrm{jets}$ data control sample), the

flavor-symmetric (FS) background predicted from eμ data events, and MC contributions from WZ/ZZ, as well as the rare SM processes with Z bosons ($t\bar{t}$Z and ZZZ, ZZW, ZWW).

In order to adapt the $\mathrm{E_T^{miss}}$ templates method to predict the Z background in these regions, we make minor modifications to the procedure used in AN-2012/254. Specifically, we re-calculate the flavor-symmetric (FS) scaling factor K and change the binning used for the $\mathrm{E_T^{miss}}$ templates. The FS background is estimated using eμ events in data. To improve the precision of this background estimate, the dilepton mass requirement is not applied, and we apply a scaling factor K, which is the efficiency for eμ events to fall in the Z mass window, extracted from MC. The values of K for various $\mathrm{E_T^{miss}}$ intervals for the high-$\mathrm{E_T^{miss}}$ region (using p_T > (20,10) GeV leptons and at least 2 jets) are shown in Fig. 1. Based on this plot we choose $K = 0.13 \pm 0.02$ for $\mathrm{E_T^{miss}}$ signal regions up to 200 GeV; for $\mathrm{E_T^{miss}}$ 200-300 GeV and $\mathrm{E_T^{miss}} > 300$ GeV we inflate the uncertainty to $K = 0.13 \pm 0.04$ and $K = 0.13 \pm 0.05$, respectively, due to the limited statistical precision. The values of K for the low-$\mathrm{E_T^{miss}}$ region (using p_T > (20,20) GeV leptons and at least 3 jets) are shown in Fig. 2. Based on this plot we choose $K = 0.14 \pm 0.02$ for $\mathrm{E_T^{miss}}$ signal regions up to 200 GeV; for $\mathrm{E_T^{miss}}$ 200-300 GeV and $\mathrm{E_T^{miss}} > 300$ GeV we inflate the uncertainty to $K = 0.14 \pm 0.03$ and $K = 0.14 \pm 0.07$, respectively. In addition, we change the jet p_T threshold for the $\mathrm{E_T^{miss}}$ templates jet multiplicity binning from 30 to 40 GeV, and change the H_T bins to (0,80,100,150,200,250,300,5000) GeV.

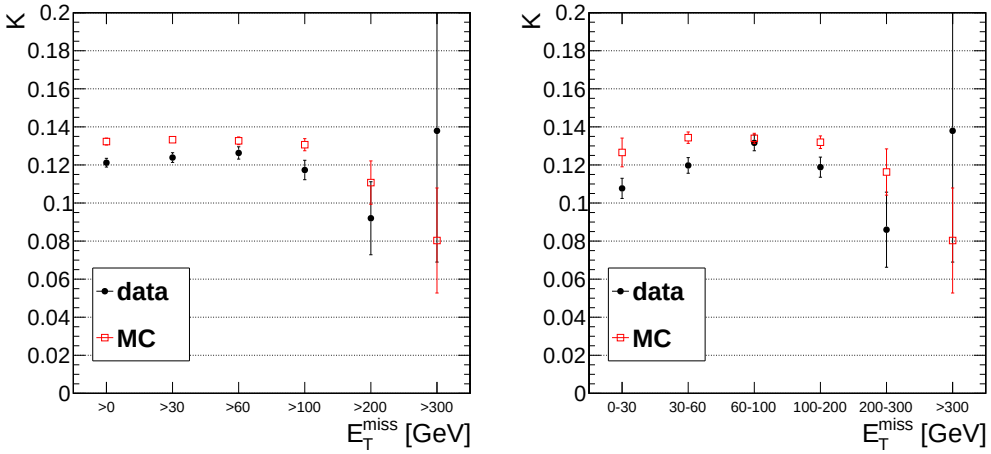

Figure 1: The efficiency for eμ events to satisfy the dilepton mass requirement, K, in data and simulation for inclusive $\mathrm{E_T^{miss}}$ intervals (left) and exclusive $\mathrm{E_T^{miss}}$ intervals (right) for the dilepton p_T > (20,10) GeV selection with at least 2 p_T > 40 GeV jets (used for the high $\mathrm{E_T^{miss}}$ signal region).

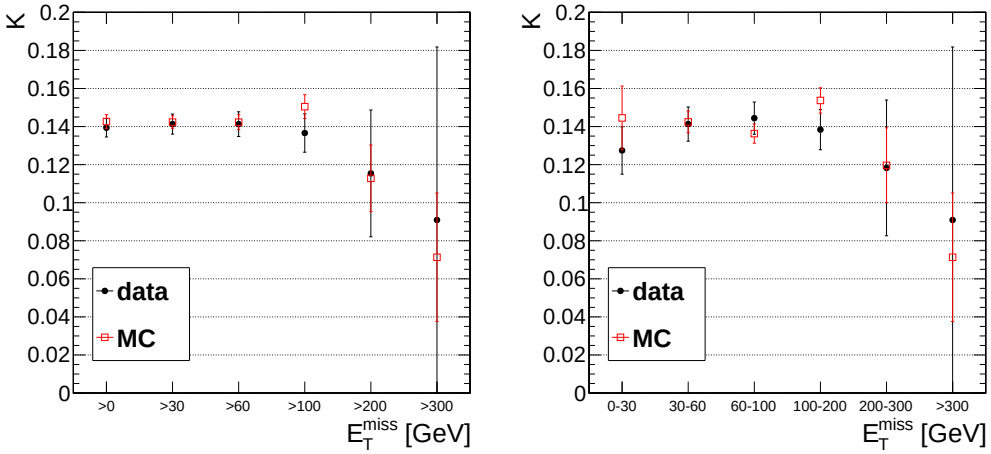

Figure 2: The efficiency for eμ events to satisfy the dilepton mass requirement, K, in data and simulation for inclusive $\mathrm{E_T^{miss}}$ intervals (left) and exclusive $\mathrm{E_T^{miss}}$ intervals (right) for the dilepton p_T > (20,20) GeV selection with at least 3 p_T > 40 GeV jets (used for the low $\mathrm{E_T^{miss}}$ signal region).

2.4 Results in Z Mass Window

The results of the low $\mathrm{E_T^{miss}}$ signal region are displayed in Fig. 3 and summarized in Table 2, separately for the Run2012A+B data (5.1 fb^{-1}) and Run2012C data (4.1 fb^{-1}). In the Run2012A+B data, we observed a 1.6σ excess for $\mathrm{E_T^{miss}} > 100$ GeV, corresponding to the low $\mathrm{E_T^{miss}}$ signal region. However, this excess does not persist in Run2012C data, where we observe good agreement between the data and the predicted background. In the combined Run2012A+B+C data (Fig. 5 and Table 4) we observe reasonable agreement over the full $\mathrm{E_T^{miss}}$ range. In the $\mathrm{E_T^{miss}} > 100$ GeV region we observe 288 events with a predicted background of 251 ± 33, representing an excess of 1.0σ.

The results of the high $\mathrm{E_T^{miss}}$ signal region are displayed in Fig. 4 and summarized in Table 3, separately for the Run2012A+B data (5.1 fb^{-1}) and Run2012C data (4.1 fb^{-1}). In both periods we observe good agreement between the data and predicted background over the full $\mathrm{E_T^{miss}}$ range. In the combined Run2012A+B+C data (Fig. 5 and Table 4) we observe reasonable agreement over the full $\mathrm{E_T^{miss}}$ range. In the $\mathrm{E_T^{miss}} > 150$ GeV region corresponding to the high $\mathrm{E_T^{miss}}$ signal region in the full sample, we observe 167 events with a predicted background of 177 ± 25 events, representing a deficit of -0.4σ.

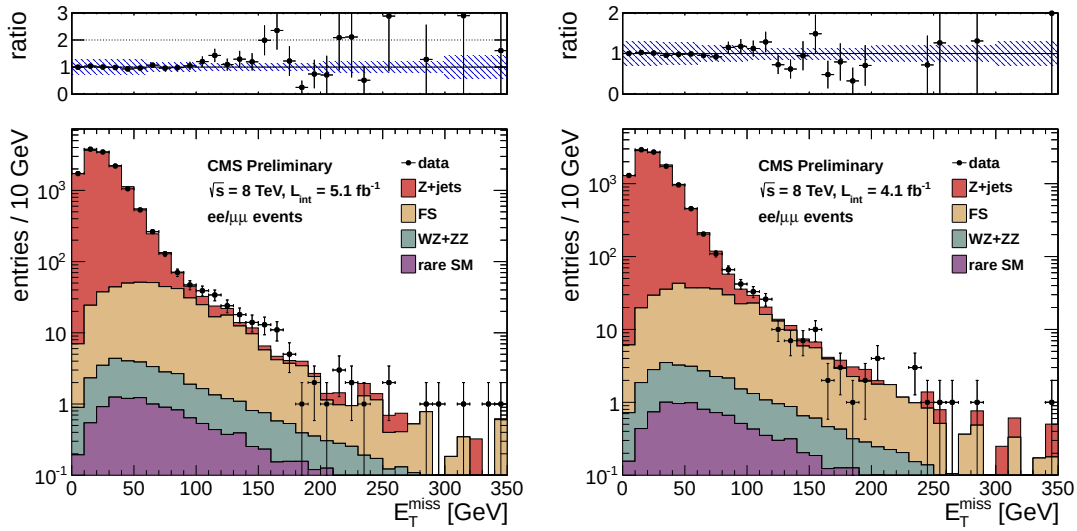

Figure 3: Results for the low $\mathrm{E_T^{miss}}$ signal region. The results for 5.1 fb^{-1} 2012A+B data are displayed on the left, the results for 4.1 fb^{-1} 2012C data are displayed on the right. The observed $\mathrm{E_T^{miss}}$ distribution (black points) is compared with the sum of the predicted $\mathrm{E_T^{miss}}$ distributions from Z+jets , flavor-symmetric backgrounds, WZ+ZZ backgrounds, and rare SM backgrounds. The ratio of observed to predicted yields in each bin is indicated. The error bars indicate the statistical uncertainty in the data and the shaded band indicates the total background uncertainty.

Table 2: Results for the low $\mathrm{E_T^{miss}}$ signal region. The results for 5.1 fb^{-1} 2012A+B data are displayed in the top table, the results for 4.1 fb^{-1} 2012C data are displayed in the bottom table. The total background is the sum of the Z + jets background predicted from the $\mathrm{E_T^{miss}}$ templates method (Z + jets bkg), the flavor-symmetric background predicted from eμ events (FS bkg), the WZ and ZZ backgrounds predicted from MC (WZ bkg and ZZ bkg) and the rare SM backgrounds. All uncertainties include both the statistical and systematic components. The Gaussian significance of the deviation between the data and total background is indicated for signal regions with at least 20 observed events.

	$\mathrm{E_T^{miss}} > 0$ GeV	$\mathrm{E_T^{miss}} > 30$ GeV	$\mathrm{E_T^{miss}} > 60$ GeV	$\mathrm{E_T^{miss}} > 100$ GeV	$\mathrm{E_T^{miss}} > 200$ GeV	$\mathrm{E_T^{miss}} > 300$ GeV
Z + jets bkg	12870 ± 3862	4118 ± 1236	356 ± 107	27.5 ± 8.5	2.6 ± 1.1	0.3 ± 0.3
FS bkg	451 ± 70	389 ± 61	256 ± 40	99.1 ± 15.8	6.9 ± 1.8	1.0 ± 0.6
WZ bkg	24.1 ± 16.9	19.5 ± 13.7	11.8 ± 8.3	5.6 ± 3.9	1.1 ± 1.0	0.2 ± 0.2
ZZ bkg	4.3 ± 2.2	3.9 ± 2.0	3.0 ± 1.5	1.9 ± 1.0	0.5 ± 0.4	0.1 ± 0.1
rare SM bkg	12.2 ± 6.1	10.5 ± 5.3	6.9 ± 3.5	3.5 ± 1.8	0.7 ± 0.6	0.2 ± 0.2
total bkg	13362 ± 3862	4541 ± 1238	634 ± 115	**138 ± 18**	11.8 ± 2.5	1.8 ± 0.8
data	13412	4461	684	**175**	14	3
significance	0.0σ	-0.1σ	0.4σ	**1.6**σ	0.5σ	

	$\mathrm{E_T^{miss}} > 0$ GeV	$\mathrm{E_T^{miss}} > 30$ GeV	$\mathrm{E_T^{miss}} > 60$ GeV	$\mathrm{E_T^{miss}} > 100$ GeV	$\mathrm{E_T^{miss}} > 200$ GeV	$\mathrm{E_T^{miss}} > 300$ GeV
Z + jets bkg	10203 ± 3061	3449 ± 1035	320 ± 97	20.5 ± 6.3	2.1 ± 0.6	0.8 ± 0.2
FS bkg	356 ± 56	307 ± 48	201 ± 32	84.5 ± 13.5	7.2 ± 1.9	0.6 ± 0.4
WZ bkg	19.4 ± 13.6	15.7 ± 11.0	9.5 ± 6.6	4.5 ± 3.2	0.9 ± 0.8	0.2 ± 0.2
ZZ bkg	3.5 ± 1.8	3.1 ± 1.6	2.4 ± 1.2	1.5 ± 0.8	0.4 ± 0.4	0.1 ± 0.1
rare SM bkg	9.8 ± 4.9	8.5 ± 4.3	5.5 ± 2.8	2.8 ± 1.5	0.6 ± 0.5	0.1 ± 0.1
total bkg	10592 ± 3062	3783 ± 1036	538 ± 102	**114 ± 15**	11.2 ± 2.2	1.8 ± 0.5
data	10587	3673	533	**113**	12	1
significance	-0.0σ	-0.1σ	-0.0σ	**-0.0**σ		

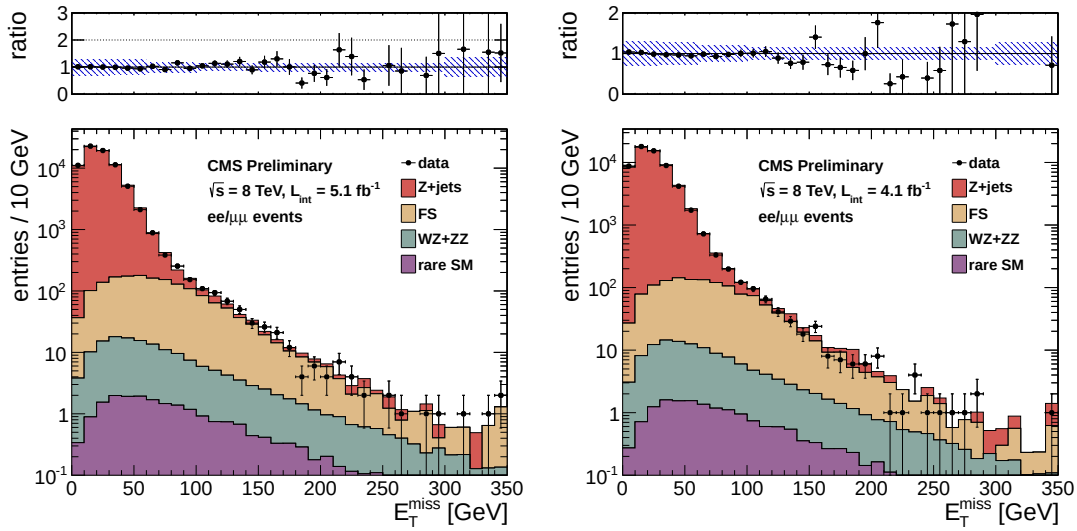

Figure 4: Results of for the high $\mathrm{E_T^{miss}}$ signal region. The results for 5.1 fb^{-1} 2012A+B data are displayed on the left, the results for 4.1 fb^{-1} 2012C data are displayed on the right. The observed $\mathrm{E_T^{miss}}$ distribution (black points) is compared with the sum of the predicted $\mathrm{E_T^{miss}}$ distributions from Z + jets , flavor-symmetric backgrounds, WZ+ZZ backgrounds, and rare SM backgrounds. The ratio of observed to predicted yields in each bin is indicated. The error bars indicate the statistical uncertainty in the data and the shaded band indicates the total background uncertainty.

Table 3: Results for the high $\mathrm{E_T^{miss}}$ signal region. The results for 5.1 fb^{-1} 2012A+B data are displayed in the top table, the results for 4.1 fb^{-1} 2012C data are displayed in the bottom table. The total background is the sum of the Z + jets background predicted from the $\mathrm{E_T^{miss}}$ templates method (Z + jets bkg), the flavor-symmetric background predicted from eμ events (FS bkg), the WZ and ZZ backgrounds predicted from MC (WZ bkg and ZZ bkg) and the rare SM backgrounds. All uncertainties include both the statistical and systematic components. The Gaussian significance of the deviation between the data and total background is indicated for signal regions with at least 20 observed events.

	$\mathrm{E_T^{miss}} > 0$ GeV	$\mathrm{E_T^{miss}} > 30$ GeV	$\mathrm{E_T^{miss}} > 60$ GeV	$\mathrm{E_T^{miss}} > 100$ GeV	$\mathrm{E_T^{miss}} > 150$ GeV	$\mathrm{E_T^{miss}} > 300$ GeV
Z + jets bkg	71975 ± 21593	19573 ± 5873	1182 ± 355	70.7 ± 21.4	13.6 ± 4.2	0.4 ± 0.4
FS bkg	1540 ± 255	1293 ± 214	823 ± 136	313 ± 52	68.6 ± 11.7	2.4 ± 1.1
WZ bkg	115.9 ± 81.2	91.8 ± 64.3	52.1 ± 36.5	22.4 ± 15.7	8.9 ± 6.3	0.8 ± 0.8
ZZ bkg	22.6 ± 11.3	20.3 ± 10.2	15.1 ± 7.6	8.8 ± 4.5	4.3 ± 2.3	0.5 ± 0.5
rare SM bkg	20.6 ± 10.3	17.9 ± 9.0	12.0 ± 6.1	6.3 ± 3.2	2.8 ± 1.5	0.3 ± 0.3
total bkg	73674 ± 21595	20996 ± 5877	2084 ± 382	421 ± 59	**98.1 ± 14.2**	4.5 ± 1.5
data	73711	20601	2121	446	**95**	4
significance	0.0σ	-0.1σ	0.1σ	0.4σ	**-0.2**σ	

	$\mathrm{E_T^{miss}} > 0$ GeV	$\mathrm{E_T^{miss}} > 30$ GeV	$\mathrm{E_T^{miss}} > 60$ GeV	$\mathrm{E_T^{miss}} > 100$ GeV	$\mathrm{E_T^{miss}} > 150$ GeV	$\mathrm{E_T^{miss}} > 300$ GeV
Z + jets bkg	57206 ± 17163	15965 ± 4790	1040 ± 313	68.3 ± 21.5	17.5 ± 6.0	1.4 ± 0.4
FS bkg	1206 ± 200	1015 ± 168	649 ± 108	244 ± 41	48.1 ± 8.3	1.3 ± 0.6
WZ bkg	93.2 ± 65.3	73.8 ± 51.7	41.9 ± 29.4	18.0 ± 12.7	7.1 ± 5.1	0.7 ± 0.7
ZZ bkg	18.2 ± 9.1	16.3 ± 8.2	12.1 ± 6.1	7.1 ± 3.6	3.4 ± 1.8	0.4 ± 0.4
rare SM bkg	16.6 ± 8.3	14.4 ± 7.2	9.7 ± 4.9	5.1 ± 2.6	2.3 ± 1.2	0.3 ± 0.3
total bkg	58541 ± 17164	17084 ± 4793	1753 ± 332	343 ± 48	**78.4 ± 11.7**	4.0 ± 1.1
data	58478	16494	1690	321	**72**	1
significance	-0.0σ	-0.1σ	-0.2σ	-0.4σ	**-0.4**σ	

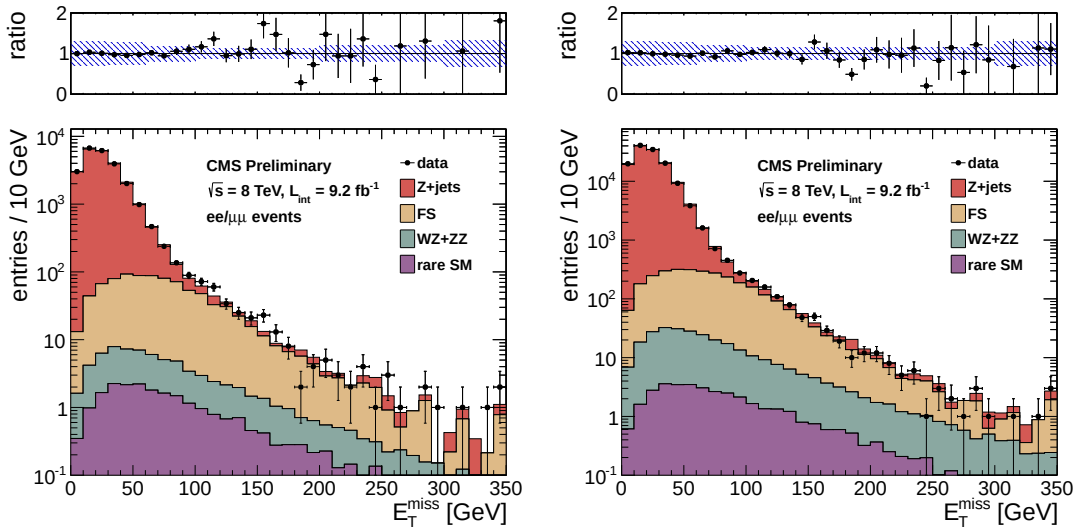

Figure 5: Results of for the low $\mathrm{E_T^{miss}}$ (left) and high $\mathrm{E_T^{miss}}$ (right) signal regions for the full 9.2 fb^{-1} sample. The observed $\mathrm{E_T^{miss}}$ distribution (black points) is compared with the sum of the predicted $\mathrm{E_T^{miss}}$ distributions from Z + jets , flavor-symmetric backgrounds, WZ+ZZ backgrounds, and rare SM backgrounds. The ratio of observed to predicted yields in each bin is indicated. The error bars indicate the statistical uncertainty in the data and the shaded band indicates the total background uncertainty.

Table 4: Results for the low $\mathrm{E_T^{miss}}$ signal region (top table) and high $\mathrm{E_T^{miss}}$ signal region (bottom table). The total background is the sum of the Z + jets background predicted from the $\mathrm{E_T^{miss}}$ templates method (Z + jets bkg), the flavor-symmetric background predicted from eμ events (FS bkg), the WZ and ZZ backgrounds predicted from MC (WZ bkg and ZZ bkg) and the rare SM backgrounds. All uncertainties include both the statistical and systematic components. The Gaussian significance of the deviation between the data and total background is indicated for signal regions with at least 20 observed events.

	$\mathrm{E_T^{miss}} > 0$ GeV	$\mathrm{E_T^{miss}} > 30$ GeV	$\mathrm{E_T^{miss}} > 60$ GeV	$\mathrm{E_T^{miss}} > 100$ GeV	$\mathrm{E_T^{miss}} > 200$ GeV	$\mathrm{E_T^{miss}} > 300$ GeV
Z + jets bkg	23072 ± 6922	7566 ± 2270	674 ± 203	47.9 ± 14.6	4.7 ± 1.6	1.1 ± 0.4
FS bkg	807 ± 126	695 ± 108	457 ± 71	184 ± 29	14.1 ± 3.4	1.5 ± 0.9
WZ bkg	43.5 ± 30.5	35.1 ± 24.6	21.3 ± 14.9	10.0 ± 7.1	1.9 ± 1.7	0.4 ± 0.4
ZZ bkg	7.8 ± 3.9	7.0 ± 3.6	5.4 ± 2.8	3.3 ± 1.8	0.9 ± 0.8	0.2 ± 0.2
rare SM bkg	22.0 ± 11.0	19.0 ± 9.6	12.4 ± 6.3	6.3 ± 3.3	1.3 ± 1.1	0.3 ± 0.3
total bkg	23952 ± 6923	8323 ± 2273	1170 ± 216	**251 ± 33**	22.8 ± 4.4	3.5 ± 1.1
data	23999	8134	1217	**288**	26	4
significance	0.0σ	-0.1σ	0.2σ	**1.0**σ	0.5σ	
	$\mathrm{E_T^{miss}} > 0$ GeV	$\mathrm{E_T^{miss}} > 30$ GeV	$\mathrm{E_T^{miss}} > 60$ GeV	$\mathrm{E_T^{miss}} > 100$ GeV	$\mathrm{E_T^{miss}} > 150$ GeV	$\mathrm{E_T^{miss}} > 300$ GeV
Z + jets bkg	129184 ± 38756	35565 ± 10670	2225 ± 668	140 ± 43	31.6 ± 10.1	1.7 ± 0.6
FS bkg	2746 ± 454	2308 ± 382	1471 ± 243	557 ± 92	117 ± 20	3.7 ± 1.6
WZ bkg	209.2 ± 146.4	165.6 ± 115.9	94.1 ± 65.9	40.5 ± 28.4	16.0 ± 11.3	1.5 ± 1.5
ZZ bkg	40.8 ± 20.4	36.6 ± 18.4	27.2 ± 13.7	16.0 ± 8.1	7.7 ± 4.1	0.9 ± 0.9
rare SM bkg	37.2 ± 18.7	32.2 ± 16.2	21.7 ± 10.9	11.4 ± 5.8	5.1 ± 2.8	0.6 ± 0.6
total bkg	132217 ± 38759	38108 ± 10678	3839 ± 714	765 ± 106	**177 ± 25**	8.4 ± 2.5
data	132189	37095	3811	767	**167**	5
significance	-0.0σ	-0.1σ	-0.0σ	0.0σ	**-0.4**σ	

2.5 Extrapolation to Low Mass to Estimate the γ^*/Z Contribution

Given a prediction for the Z background in the Z mass window, we can extrapolate to estimate the low mass γ^*/Z contribution. We extract the ratio $R_{low/in}$ of low-mass to on-shell Z events from data, correcting for the contribution from flavor-symmetric backgrounds, according to:

$$R_{low/in} = (N_{SF}^{low} - N_{OF}^{low})/(N_{SF}^{in} - N_{OF}^{in}). \quad (1)$$

Here SF and OF refer to the same-flavor and opposite-flavor data yields in the "low" ($15 < m_{\ell\ell} < 70$ GeV) and "in" ($81 < m_{\ell\ell} < 101$ GeV) dilepton mass regions. To predict the low-mass γ^*/Z contribution, we scale the total predicted Z background by this quantity, which is displayed in Fig. 6. Here we measure $R_{low/in}$ in several $\mathrm{E_T^{miss}}$ regions, and assess the uncertainty based on the variation with respect to $\mathrm{E_T^{miss}}$. Based on this plot we choose

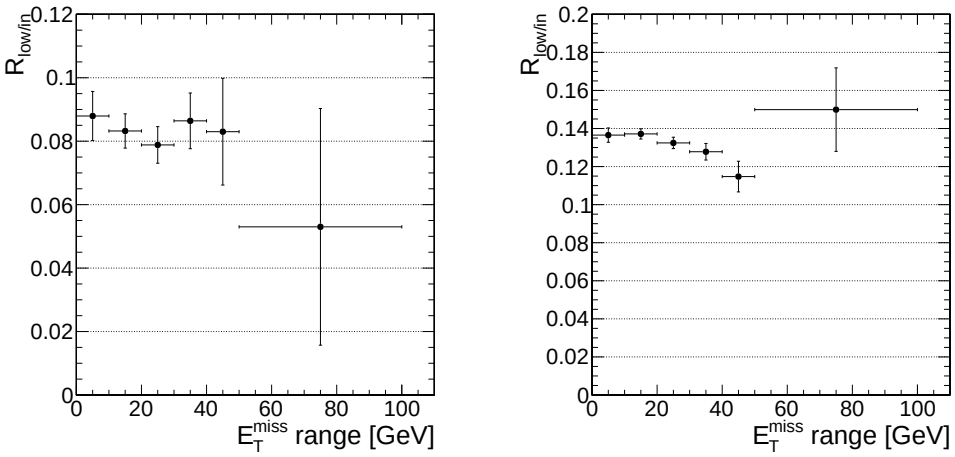

Figure 6: The ratio $R_{low/in}$ of low mass ($15 < m_{\ell\ell} < 70$ GeV) to on-Z ($81 < m_{\ell\ell} < 101$ GeV) events, as a function of the $\mathrm{E_T^{miss}}$ requirement. The left plot corresponds to the low $\mathrm{E_T^{miss}}$ signal region (2 $p_T > 20$ GeV leptons with at least 3 jets), the right plot corresponds to the high $\mathrm{E_T^{miss}}$ signal region ($p_T >$ (20,10) GeV leptons with at least 2 jets).

$R_{low/in} = 0.08 \pm 0.02$ for the low $\mathrm{E_T^{miss}}$ signal region and $R_{low/in} = 0.13 \pm 0.03$ for the high $\mathrm{E_T^{miss}}$ region.

We find the following results for the first 5.1 fb^{-1}. For the low $\mathrm{E_T^{miss}}$ signal region, the total predicted Z background in the Z mass region is 39 ± 9.6 (sum of the $\mathrm{Z} + \mathrm{jets}$, WZ+ZZ, and rare SM backgrounds from Table 2, $\mathrm{E_T^{miss}}$ > 100 GeV region), resulting in a γ^*/Z prediction of 3.1 ± 1.1 events. For the high $\mathrm{E_T^{miss}}$ signal region, the total predicted Z background in the Z mass region is 30 ± 8.1 (sum of the $\mathrm{Z} + \mathrm{jets}$, WZ+ZZ, and rare SM backgrounds from Table 3, $\mathrm{E_T^{miss}} > 150$ GeV region), resulting in a γ^*/Z prediction of 3.8 ± 1.4 events.

We find the following results for the full 9.2 fb^{-1}. For the low $\mathrm{E_T^{miss}}$ signal region, the total predicted Z background in the Z mass region is 68 ± 17 (sum of the $\mathrm{Z} + \mathrm{jets}$, WZ+ZZ, and rare SM backgrounds from Table 4, $\mathrm{E_T^{miss}}$ > 100 GeV region), resulting in a γ^*/Z prediction of 5.4 ± 1.9 events. For the high $\mathrm{E_T^{miss}}$ signal region, the total predicted Z background in the Z mass region is 60 ± 16 (sum of the $\mathrm{Z} + \mathrm{jets}$, WZ+ZZ, and rare SM backgrounds from Table 4, $\mathrm{E_T^{miss}} > 150$ GeV region), resulting in a γ^*/Z prediction of 7.9 ± 2.7 events.

2.6 Summary of Results

In this section we summarize the results for the 5.1 fb^{-1} Run2012A+B data (Table 5) and the 9.2 fb^{-1} Run2012A+B+C data (Table 6).

Table 5: Summary of results in 5.1 fb^{-1} 2012A+B data for the low-$\mathrm{E_T^{miss}}$ and high-$\mathrm{E_T^{miss}}$ signal regions (SR). In the Z mass region, the predicted Z background (Z bkg, sum of Z + jets , WZ/ZZ, and rare SM processes with Z bosons), flavor-symmetric background (FS bkg), and total background (Total bkg) are indicated, and compared to the observed yield (Data). The Gaussian significance of the difference between the data and the total background is indicated. The predicted γ^*/Z contribution to the low-mass region (Low mass γ^*/Z bkg) is also indicated.

	Low-$\mathrm{E_T^{miss}}$ SR	High-$\mathrm{E_T^{miss}}$SR
Z bkg	39 ± 9.6	30 ± 8.1
FS bkg	99 ± 16	69 ± 12
Total bkg	138 ± 18	98 ± 14
Data	175	95
Significance	$+1.6\sigma$	-0.2σ
Low mass γ^*/Z bkg	3.1 ± 1.1	3.8 ± 1.4

Table 6: Summary of results in 9.2 fb^{-1} 2012A+B+C data for the low-$\mathrm{E_T^{miss}}$ and high-$\mathrm{E_T^{miss}}$ signal regions (SR). In the Z mass region, the predicted Z background (Z bkg, sum of Z + jets , WZ/ZZ, and rare SM processes with Z bosons), flavor-symmetric background (FS bkg), and total background (Total bkg) are indicated, and compared to the observed yield (Data). The Gaussian significance of the difference between the data and the total background is indicated. The predicted γ^*/Z contribution to the low-mass region (Low mass γ^*/Z bkg) is also indicated.

	Low-$\mathrm{E_T^{miss}}$ SR	High-$\mathrm{E_T^{miss}}$SR
Z bkg	68 ± 17	60 ± 16
FS bkg	184 ± 29	117 ± 20
Total bkg	251 ± 33	177 ± 25
Data	288	167
Significance	$+1.0\sigma$	-0.4σ
Low mass γ^*/Z bkg	5.4 ± 1.9	7.9 ± 2.7

3 Cross-check with single lepton triggers

The nominal "edge analysis" is performed with dilepton triggers. An excess of SF vs. OF events may thus be observed if there were some inefficiency for the eμ triggers used in this analysis. In this section we provide a cross-check of the nominal analysis by including events collected with single lepton triggers. The relevant triggers are:

- ee channel
  - dilepton: `HLT_Ele17_CaloIdT_CaloIsoVL_TrkIdVL_TrkIsoVL_Ele8_CaloIdT_CaloIsoVL_TrkIdVL_TrkIsoVL`
  - single lepton: `HLT_Ele27_WP80`
- $\mu\mu$ channel
  - dilepton: `HLT_Mu17_Mu8` OR `HLT_Mu17_TkMu8`
  - single lepton: `HLT_IsoMu24` OR `HLT_IsoMu24_eta2p1`
- $e\mu$ channel
  - dilepton: `HLT_MuX_EleY_CaloIdT_CaloIsoVL_TrkIdVL_TrkIsoVL` (X,Y=17,8 OR 8,17)
  - single lepton: `HLT_Ele27_WP80` OR `HLT_IsoMu24` OR `HLT_IsoMu24_eta2p1`

In the nominal analysis based on dilepton triggers only, an ee event is required to satisfy the ee dilepton trigger, a $\mu\mu$ event is required to satisfy one of the two $\mu\mu$ dilepton triggers, and an eμ event is required to satisfy one of the two eμ dilepton triggers. Here we compare the results obtained from the nominal dilepton triggers with those obtained by requiring an OR of the dilepton and single lepton triggers. In this cross-check, an ee event is required to satisfy the ee dilepton trigger OR single electron trigger, a $\mu\mu$ event is required to satisfy one of the two $\mu\mu$ dilepton triggers OR one of the two single muon triggers, and an eμ event is required to satisfy one of the two eμ dilepton triggers OR the single electron trigger OR the single muon trigger. The results are summarized in Table 7. Including the single lepton triggers increases the yields in the ee, $\mu\mu$ and eμ final states by (1–7)%, and does not significantly alter the excess of SF vs. OF data yields.

Table 7: Summary of results comparing dilepton vs. dilepton OR single lepton triggers, for 5.1 fb^{-1}, in the low $\mathrm{E_T^{miss}}$ and high $\mathrm{E_T^{miss}}$ signal regions (SR). The ratio of the dilepton OR single lepton yield to the dilepton only yield is indicated, along with the excess of SF w.r.t. OF events.

Region	N_{ee}	$N_{\mu\mu}$	$N_{\mathrm{e}\mu}$	$N_{\mathrm{ee}} + N_{\mu\mu} - N_{\mathrm{e}\mu}$
Low $\mathrm{E_T^{miss}}$ SR and $20 < m_{\ell\ell} < 70$ GeV				
dilepton (nominal)	106	153	189	70 ± 21.2 (stat)
dilepton OR single lepton	112	155	199	68 ± 21.6 (stat)
ratio	1.06	1.01	1.05	
Low $\mathrm{E_T^{miss}}$ SR and $m_{\ell\ell} > 20$ GeV				
dilepton (nominal)	357	517	693	181 ± 39.6 (stat)
dilepton OR single lepton	368	534	739	163 ± 40.5 (stat)
ratio	1.03	1.03	1.07	
High $\mathrm{E_T^{miss}}$ SR and $15 < m_{\ell\ell} < 70$ GeV				
dilepton (nominal)	89	157	187	59 ± 20.8 (stat)
dilepton OR single lepton	93	160	197	56 ± 21.2 (stat)
ratio	1.04	1.02	1.05	
High $\mathrm{E_T^{miss}}$ SR and $m_{\ell\ell} > 15$ GeV				
dilepton (nominal)	258	380	527	111 ± 34.1 (stat)
dilepton OR single lepton	271	386	553	104 ± 34.8 (stat)
ratio	1.05	1.02	1.05	

Next, we compare the results obtained with the dilepton triggers to results obtained with single lepton triggers only. Since the single electron (single muon) triggers have p_T thresholds of 27 (24) GeV, we use a dilepton $p_T >$ (30,20) selection. The results are summarized in Table 8. Switching from dilepton to single lepton triggers alters the yields by (-2–5)%, and does not significantly alter the excess of SF vs. OF data yields.

Table 8: Summary of results comparing dilepton vs. single lepton triggers (with a dilepton $p_T >$ (30,20) GeV selection, for 5.1 fb^{-1}, in the low $\mathrm{E_T^{miss}}$ and high $\mathrm{E_T^{miss}}$ signal regions (SR). The ratio of the single lepton trigger yield to the dilepton trigger yield is indicated, along with the excess of SF w.r.t. OF events.

Region	N_{ee}	$N_{\mu\mu}$	$N_{\mathrm{e}\mu}$	$N_{\mathrm{ee}} + N_{\mu\mu} - N_{\mathrm{e}\mu}$
Low $\mathrm{E_T^{miss}}$ SR and $20 < m_{\ell\ell} < 70$ GeV				
dilepton	95	135	169	61 $\pm$ 20.0 (stat)
single lepton	93	134	172	55 $\pm$ 20.0 (stat)
ratio	0.98	0.99	1.02	
Low $\mathrm{E_T^{miss}}$ SR and $m_{\ell\ell} > 20$ GeV				
dilepton	345	497	669	173 $\pm$ 38.9 (stat)
single lepton	346	499	700	145 $\pm$ 39.3 (stat)
ratio	1.00	1.00	1.05	
High $\mathrm{E_T^{miss}}$ SR and $15 < m_{\ell\ell} < 70$ GeV				
dilepton	48	72	79	41 $\pm$ 14.1 (stat)
single lepton	47	72	81	38 $\pm$ 14.1 (stat)
ratio	0.98	1.00	1.03	
High $\mathrm{E_T^{miss}}$ SR and $m_{\ell\ell} > 15$ GeV				
dilepton	197	270	367	100 $\pm$ 28.9 (stat)
single lepton	200	269	377	92 $\pm$ 29.1 (stat)
ratio	1.02	1.00	1.03	

References

[1] CMS Collaboration, "Search for physics beyond the standard model in events with a Z boson, jets, and missing transverse energy in pp collisions at $\sqrt{s} = 7$ TeV,", arXiv:1204.3774v1 [hep-ex].